Organic & Biomolecular Chemistry

Accepted Manuscript

ROYAL SOCIETY OF CHEMISTRY

www.rsc.org/obc

Journal Name Organic & Biomolecular Chemistry Dynamic Article Links ►

Cite this: DOI: 10.1039/c0xx00000x

www.rsc.org/xxxxxx

ARTICLE TYPE

Using Computational Methods to Explore Improvements on Knölker's Iron Catalyst

Xi Lu,[a] Yawei Zhang,[b] Nicholas Turner,[c] Mingtao Zhang*[b] and Tonglei Li*[d]

Received (in XXX, XXX) Xth XXXXXXXXX 20XX, Accepted Xth XXXXXXXXX 20XX
DOI: 10.1039/b000000x

Abstract: Knölker's iron catalyst is characterized by low toxicity and its relatively low price in comparison to precious metal catalysts. Density functional theory was used to explore improvements on this catalyst. It was found that electron-withdrawing substituent on the CpOH ring is favorable to improve the efficiency of iron catalysts. Increasing the acidity of CpOH is also an available means for improving the catalytic efficiency. However, replacing the hydroxyl of CpOH with the amino group is not a valid choice. In contrast, substituting phosphine ligands for carbonyls is the most effective method for improving the catalytic activity of the iron catalyst. But, the PR_3 ligand must have electron-donating groups and its steric effect should be controlled in a suitable range. Replacing carbonyl groups by PH_3 and $PPhH_2$ ligands can effectually improve the catalytic activity for hydrogenation of ketones.

Introduction

The iron-based complex, as a highly efficient catalyst, is widely applied in homogeneous hydrogenations of C=C bonds, nitroaromatics and aryl azides.[1] However, there has been little application of iron complexes for the catalytic hydrogenation of ketones and aldehydes in the past decades.[2,3] Although the iron-based complex $[Ph_4(\eta^4\text{-}C_4CO)]Fe(CO)_3$ was once used to catalyze reduction of ketones in 1958, it shows very little catalytic activity and decomposes to produce a heterogeneous mixture under the conditions used when exploring hydrogenation of ketones in aqueous THF.[4,5]

Since the discovery of Shvo's catalyst in the mid-1980s,[6] ligand-metal bifunctional complexes of precious metals (Ru, Rh, Ir and Os) as major catalysts have been largely used for hydrogenation of polar multiple bonds.[7,8,9] But toxicity and high prices limit the availability of catalysts of noble metal in industry.[2,10] By comparison, the iron-based complex is a proper substitute due to features like low cost, low toxicity and high abundance.[3,11] There are already many natural iron-based catalysts such as hydrogenase for reduction.[12] Recently, Casey and Guan[13] successfully demonstrated that Knölker's iron-based complex[14] is a very efficient catalyst for the hydrogenation of aldehydes and aldimines even under mild conditions (low H_2 pressure and room temperature), and it also has a high chemoselectivity for ketones with unconjugated C=C or C≡C where only the ketone is hydrogenated. However, Knölker's catalyst can not show a relatively high catalytic activity and enantioselectivity for hydrogenation of ketones in Casey's studies.[13]

Scheme 1 Shvo's[15] and Knölker's[14] Catalysts

Improvements to Knölker's catalyst are gradually becoming an interesting topic in catalysis of hydrogenation of aldehydes and ketones.[1a,3] Williams *et al.*[16] and Wills *et al.*[17] separately reported some novel iron complexes (in scheme 2) via Knölker's synthetic method[14], and they also successfully applied them to the hydrogenation of ketones. More recently, Casey and Guan[18] synthesized an iron-based derivative which can catalyze the hydrogenation of aldehydes and ketones. However, none of these modified iron complexes showed a higher activity than Knölker's catalyst for the catalytic hydrogen transfer of aldehydes and ketones, according to kinetic studies.[17,18]

Scheme 2 Some Improved Iron-based Complexes

Experimentally, the modification for Knölker's catalyst is limited to a large extent, due to some confessed difficulties, such as the synthesis of the organometallic complex, the selection of reaction conditions, etc. In this case, computational methods can be considered as a functional and reliable means. They once helped experiments to reasonably explain the hydrogenation process of aldehydes and ketones, which is an outer-sphere converted hydrogen-transfer mechanism. The computational results were also in well agreement with Shvo's and Casey's experimental proposals.[13,19-28] So, density functional theory was used to perform a deeply detailed theoretical study for improvements to Knölker's catalyst in this paper. These computational results are expected to supply some reasonable and available suggestions to the experimental improvement of the iron-based catalyst in order to increase the catalytic activity for hydrogen transfer of aldehydes and ketones.

Computational details

Calculations for all systems were carried out using the Gaussian 09 software package[29] at the density functional theory (DFT) level of the hybrid B3LYP[30] functional and LACVP* basis set. The effective core potential LANL2DZ[31] along with its associated basis set was employed for Fe and the main group elements (C, O, H, P, F, N and Si) were calculated using the 6-31G* basis set.

All calculations were done without any geometrical constraints in gas phase. Frequency calculations were performed for all stationary points at the same level in order to identify the minima (zero imaginary frequency) and transition states (TS, only one imaginary frequency) and to provide free energies at 298.15 K and 1 atm. Intrinsic reaction coordinate (IRC)[32] analysis was carried out to confirm that all stationary states were smoothly connected to each other. Solvent effects (in toluene) were included using the SMD model[33,34] (as implemented in Gaussian 09) by performing single-point calculations in toluene via B3LYP-optimized gas-phase geometries at a higher level of 6-311+G* basis set for all elements with the M06 method. This method was reported by Zhao and Truhlar[35,36] that had a high accuracy for the calculation of the thermochemistry and kinetics of transition metals and main-group elements.

Furthermore, a correction term of 1.8943 kcal/mol has to be added to the *G*(sol) calculations, to convert the gas-phase standard free energies at a standard state of 1 atm to the appropriate standard state for a solution of 1 mol/L.[37,38] Since the iron-catalyzed hydrogenation of formaldehyde is a bimolecular reaction, the transition state can cause an entropy penalty in this step. So free energies ΔG(sol) were adopted to evaluate efficiencies of improved iron catalysts in this paper.

Results and Discussion

The benchmark between calculation and experiment.

The catalytic efficiency of Knölker's iron complex was investigated primarily in order to establish a benchmark for improvements. The parameters for the iron-catalyst, [2,5-$(SiMe_3)_2$-3,4-$(CH_2)_4(\eta^5$-$C_4COH)$]$Fe(CO)_2H$, **1a**, used in the calculations were obtained from its X-ray crystal structure.[14c] The entire aromatic ligand of the catalyst is hereafter referred to as CpOH. The benzaldehyde PhCHO was selected as the substrate in this paper due to a kinetic study performed in Casey's experiment. Hence, the calculations match experimental conditions well, and the computational results may be applied and compared to experiments.

For the hydrogenation of aldehydes, an outer-sphere concerted hydrogen-transfer mechanism (see scheme 3) has been demonstrated to be the most kinetically favorable pathway in theoretical and experimental studies.[13,27,28] In this catalytic hydrogenation, the substrate PhCHO and catalyst **1a** first interact to form intermediate **3a** through transition state **2aTS** which corresponds to a concerted hydrogen-transfer mechanism. Intermediate **3a** is a complex composed of **4a** and an alcohol using a Fe⋯H agostic interaction and a hydrogen bond between the oxygen of the Cp group and the hydroxy hydrogen. Intermediate **4a** and a free alcohol can be obtained by the further dissociation of intermediate **3a**. Finally, **4a** and alcohol connect again to produce complex **5a**. The hydrogenated product **5a** can be regenerated to catalyst **1a** through a reduction reaction in the presence of H_2. In previous DFT calculations, the hydrogen transfer was suggested to be a rate-determining step in the catalytic cycle. [27]

Scheme 3 Hydrogenation mechanism of PhCHO catalyzed by Knölker's Fe-catalyst **1a**

Based on this mechanism, a free energy barrier of 14.5 kcal/mol was obtained for the hydrogenation of PhCHO catalyzed by Knölker's catalyst (see Fig.1). It is higher than the calculated barrier of 8.9 kcal/mol for hydrogenation of formaldehyde,[28] because the phenyl group donates electrons to the C=O bond.[39] The dissociation of **3a** was endergonic by only 4.4 kcal/mol and gave rise to **4a** and the free $PhCH_2OH$. However, the separated **4a** is thermodynamically unstable and it can quickly connect to $PhCH_2OH$ again to form complex **5a**. As shown in Fig.2, the distances of Fe⋯O and O⋯H are 2.068 Å and 1.713 Å in the structure of **5a**, and separately correspond to the stronger σ-coordinated and hydrogen bonding interactions between the catalyst and alcohol. The optimized structure of **5a** in calculation is very consistent with the X-ray crystal obtained in experiment (Table S1 and S2 of SI). It was exoergic by 16.3 kcal/mol for **4a** + $PhCH_2OH$ → **5a** reaction. This indicates that complex **5a**, rather than **4a** and free $PhCH_2OH$ is the final product, which is also in agreement with Casey's experimental conclusion.[23]

Fig. 1 Free energy ΔG(sol) profile for hydrogenation of PhCHO catalyzed by **1a** obtained at the M06/6-311+G* level in toluene (kcal/mol). Relative to free energies of **1a** and PhCHO.

Hydrogenation of PhCHO is still kinetically very favorable and corresponds to a highly rapid reaction rate, which indicates that Knölker's catalyst has a high catalytic efficiency for the hydrogen transfer to PhCHO. This is in agreement with Casey and Guan's experimental result where they found the reduction of PhCHO has a very rapid rate at 25 ºC.[18] This means that a valid modification must have a lower barrier than 14.5 kcal/mol for the catalytic hydrogen transfer of PhCHO, because the total free energy barrier plays a crucial role in the catalytic cycle.[40]

Fig. 2 Optimized structures for hydrogenation of PhCHO catalyzed by **1a**. Distances in Å. FeCOH indicates the dihedral angle. All hydrogen atoms connected to carbons in the CpOH ring were ignored.

Based on our previous studies for the exclusive transition state **2aTS** in this mechanism,[28] the hydrogenation can be achieved when the H^+ cation of the CpOH group and H^- anion of an Fe-H bond concertedly transfer to the oxygen and carbon atoms of the C=O bond of aldehyde. So, the following improvements that aimed to increase the efficiency of the catalyst were carried out by means of some other special groups replacing the original substituents and ligands (see Scheme 4), in order to change the polarization of the CpO-H or Fe-H bonds of Knölker's catalyst to make hydrogen transfer more favorable.

Scheme 4 Designed modifications for the Knölker's catalyst

Improving Knölker's catalyst by changing the substituent groups of CpOH ring.

In this section, the CpOH group was first modified considering the experimental improvements to Shvo's catalyst. As the type i presented in Scheme 4, the original substituents of CpOH were replaced by some other functional group like methyl groups, phenyl groups, and fluoro atoms. Then, the electronic density of the conjugated π-bond of cyclopentadienyl can be changed, in order to generate an influence on the polarization of the CpO-H bond. Fig. 3 shows that the substituent of the CpOH group corresponds to a methyl group, phenyl group, and fluorine atom in iron-complexes **1b**, 1c and **1d**, respectively. These optimized structures are very similar to the geometry of **1a**, where the CpOH group has a η^5-coordinated interaction with iron. However, dihedral angles of **1c** and **1d** were slightly increased relative to that of **1a** and **1b**, due to a decreased steric effect of the phenyl and the F atom.

Fig. 3 Optimized structures for hydrogenation of PhCHO catalyzed by **1b, 1c** and **1d**. Distances in Å. FeCOH indicates the dihedral angle. Hydrogen atoms of the CpOH ring were ignored for only transition states here.

Table 1 shows that the hydrogenation of **1b +** PhCHO → **5b** is exoergic by 5.4 kcal/mol, which means product **5b** exhibits a higher thermodynamic stability relative to **5a**. However, there is little difference in the hydrogenation barrier of PhCHO catalyzed by **1b** compared with **1a**, 14.4 versus 14.5 kcal/mol. This is because the electron donation of methyl is similar to the original substituents, $SiMe_3$ and $-(CH_2)_4-$. A better electron-donating group, phenyl, was then used in **1c**, but the barrier slightly increased (by 0.1 kcal/mol). Moreover, the hydrogenation catalyzed by **1c** became less thermodynamically favorable, due to **1c +** PhCHO → **5c** being exoergic by 4.2 kcal/mol. The results of these two modifications indicate that the electron-donating substituent did not provide an efficient improvement to the iron-based catalyst. In summary, the steric factors of methyl and phenyl are obviously less than that of $SiMe_3$, but the barriers have little difference. This demonstrates that the steric hindrance of the substituent of CpOH has little influence on the catalyst's efficiency.

Table 1 Free energy ΔG(sol) profiles for hydrogenation of PhCHO catalyzed by improved catalysts **1b, 1c** and **1d** obtained at the M06/6-311+G* level in toluene (kcal/mol).

For complex **1d**, the substituent was changed to the fluorine atom, which possesses strong electron-withdrawing power. Here, the free energy of activation was reduced to 13.5 kcal/mol for transition state **2dTS**, which is 1.0 kcal/mol lower than **1a**'s barrier. According to Eyring equation, the catalytic efficiency of **1d** is advanced 8 times relative to **1a**. At the same time, the free energy was also decreased to -9.4 kcal/mol for product **5d**. Furthermore, free energies of intermediate **3d** and **4d** were also to some extent decreased. These results show that complex **1d** is more kinetically and thermodynamically favorable to catalyze hydrogen transfer. For these three improvements, only **1d** shows a lower barrier for hydrogenation, which means that adding electron-withdrawing substituents to CpOH is favorable in increasing the efficiency of the iron-based catalyst.

Amino-groups replacing the hydroxyl of CpOH.

In this section, improvements on the OH of the CpOH group were explored. The above modifications aimed to indirectly influence the hydroxyl by changing the electronegativity of the CpOH ring. Here, the hydroxyl was directly improved by means of using the amino group as a substituent (see the type ii in Scheme 4). The amino group was experimentally a typical replacement of the hydroxyl,[9] because NR′H has the advantage that one hydrogen can be replaced by other groups like H, CH_3, Ph and F.

As shown in Fig.4, the conformation of **1e** and **1h** is similar to that of **1a**, because the steric effects of the hydrogen and fluorine atoms are insignificant. However, the FeCNR′ dihedral angles of **1f** and **1g** are 174.9º and 172.8º, respectively, indicating that the R′ is located nearly in the middle of two $SiMe_3$ groups. This geometry can avoid, to a large extent, the steric hindrance between R′ (methyl or phenyl) and $SiMe_3$ groups.

Fig.4 Optimized structures for hydrogenation of PhCHO catalyzed by **1e, 1f, 1g** and **1h** and the dihedral angles. Distances in Å.

Table 2 shows that the barrier of **2eTS** is 25.4 kcal/mol, where the NH_2 group, replaced the hydroxyl of the CpOH group, only caused a little steric factor with two $SiMe_3$ groups. For **2fTS** and **2gTS**, the barriers are 27.6 and 30.2 kcal/mol, respectively, which shows an increasing trend for adding the electron donating ability of R′ substituents. This result is also in agreement with the experimental modifications on ruthenium catalysts.[21] When R′ was changed to a fluorine atom with powerful electron-withdrawing capability, the barrier of **2hTS** declined to 19.5 kcal/mol. Here, none of the three improvements show a lower barrier than **2aTS**. There are two reasons leading to these unexpected results, which are similar to the expectation of Casey[21] for ruthenium complex. First, the NR′H group has a lower acidity compared with the hydroxyl. Adding the electron donation of R′ can further reduce the acidity of NR′H and causes a higher barrier for hydrogenation, such as in **2fTS** and **2gTS**. However, even when the fluorine was used to increase the acidity of NR′H, the barrier of **2hTS** was still 5.0 kcal/mol higher than that of **2aTS**. All these show that the amino group is unfavorable to donate a proton to aldehyde in hydrogen transfer. Second, there is a significant steric effect in these transition states. Fig.4 shows that the R′ substituent is closer to the plane of the Cp ring in the transition states, due to the maximum dihedral angle being only 54.4º. As a result, these structural changes induce a greater steric hindrance between the substituent and $SiMe_3$ group. These two factors largely restricted the increase of the catalytic efficiency for these iron-complexes with amino substituents.

Table 2 Free energy ΔG(sol) profiles for hydrogenation of PhCHO catalyzed by modifications **1e, 1f, 1g** and **1h** obtained at the M06/6-311+G* level in toluene (kcal/mol).

The CNCC dihedral angles of products **5e**, **5f**, **5g** and **5h** show that the torsion of R′ groups to some extent breaks the conjugation of N=C double bonds. Simultaneously, a steric effect also exists between of R′ and $SiMe_3$ groups for these products. This caused the thermodynamic stabilization to be greatly reduced. Free energies of these products correspond to 14.1, 17.1, 16.8 and 0.4 kcal/mol, respectively. So, it is thermodynamically unfeasible to hydrogenate an aldehyde using catalysts **1e**, **1f**, and **1g**. Only **1h** is thermodynamically feasible for the catalytic hydrogen transfer of aldehydes.

Based on these discussions, replacing the hydoxyl group of CpOH with the amino group is not a valid improvement upon Knölker's catalyst. However, these results show that increasing the acidity of the OH group is an available and effective method for improving catalytic activity. To achieve this, the hydrosulphonyl is suggested as a potential substitute for the hydroxyl group, which will be studied in our future calculations.

Substituted phosphine ligands for carbonyls.

All above modifications mainly aimed to increase the acidity of the CpOH ring in order to improve the catalytic activity of iron catalysts. Increasing the hydride donor ability of Fe-H is another potential way to enhance the efficiency of catalysts. A feasibility study on this improvement was performed in this part by means of replacing the CO ligand with the phosphine ligand. In particular, PH_3, PMe_3, PPh_3 and PF_3 were used (see the type iii in Scheme 4).

As shown in Fig.5, there are three conformations for these improved complexes, due to the influence of steric effects between the phosphine ligand and the CpOH group. For **1i** and **1j**, the PH_3 and $PPhH_2$ ligands have less steric factors, but the hydroxylic hydrogen of the CpOH group still underwent a rotation towards the other side relative to that of **1a**. Complex **1k** is similar to **1f** and **1g**, where the hydrogen of OH is located nearly in the middle of two $SiMe_3$ groups (dihedral angle FeCOH = 5.8º) to avoid adding significant steric hindrance between the CpOH group and PMe_3 ligands. Complex **1l** also exhibits an intramolecular steric hindrance, but it still has a semblable geometry with **1a**. This is because there are many intramolecular hydrogen bonding interactions between the CpOH group and PF_3 ligands in the structure of **1l**, where some F⋯H distances are in the range of 2.504 to 2.666 Å. Thus, these interactions compensated for the steric hindrance, and improved the stability of **1l** to a large extent.

Fig.5 Optimized structures for **1i, 1j, 1k** and **1l** catalyzed hydrogenation of PhCHO and the dihedral angles. Distances in Å.

Table 3 shows that there is an increasing tendency for the barrier of **2iTS**, **2jTS** and **2kTS**. Comparing structures of **2iTS**, **2jTS** and **2kTS** (see Figure5), the distances of Fe⋯H are 1.618, 1.633 and 1.660 Å, respectively; simultaneously, the distances of H⋯C(HPh)=O are 1.457,1.463 and 1.534 Å, respectively. This demonstrates that the distance between the iron catalyst and PhCHO is elongated due to the increase in the steric effect of the phosphine ligand, especially for $PPhH_2$ and PMe_3. The **2jTS** geometry exhibits a steric hindrance between the PhCHO and the phenyl of $PPhH_2$, upon approaching the hydride ion of the iron catalyst. Also this steric hindrance was further increased in **2kTS**, as the PMe_3 ligand has a very significant steric effect. Thus, adding the steric effects of the phosphine ligand leads to the increase of the barrier for the iron catalyzed hydrogenation of aldehyde. However, all of these barriers are lower than the 14.5 kcal/mol of **2aTS**, because PH_3, PPh_3, and $PhMe_3$ groups have an electron-donating capability which can efficiently increase the coordinated ability of phosphine ligand. This factor is more favorable in the hydride transfer and exceeds the influence of steric hindrance, so the barrier is reduced for the catalytic hydrogen transfer of an aldehyde.

Table 3 Free energy ΔG(sol) profiles for hydrogenation of PhCHO catalyzed by modified catalysts **1i, 1j, 1k** and **1l** obtained at the M06/6-311+G* level in toluene (kcal/mol).

Then, PF_3 was used for a substituent ligand in **1l**, which was expected to deliver a more effective improvement. This ligand has a similar steric effect as the PH_3 ligand, but its coordinated ability is largely reduced by the electrophilic effect of the fluorine atom. As a result, the hydride becomes more difficult to dissociate from the Fe-H bond, which leads to an increase in the barrier of **1lTS** of 17.7 kcal/mol. The distance of Fe⋯O is shortened to 2.088 Å in the product **5l** compared to the 2.102 Å of **5i**, 2.113 Å of **5j** and 2.154 Å of **5k**. The lower capability of coordination of PF_3 is unfavorable to the iron achieving the 18 *d*-electron structure in **5l**, so benzyl alcohol has to be closer to the catalyst in order to donate electrons to the iron atom. Thus, more steric hindrance is observed between benzyl alcohol and the PF3 ligands in **5l**, which caused the thermodynamic stabilization of **5l** to be largely reduced. Here, the **1l** + PhCHO → **5l** reaction is exoergic by 0.3 kcal/mol.

Overall, these results show that the PR_3 ligand with an electron-donating group coordinated to iron is able to improve the catalytic activity of the iron catalyst. The steric factor of PR_3 ligand should be limited in a proper range. The PR_3 ligand with an electron-withdrawing group used for a ligand did not present any kinetic or thermodynamic improvements to the iron catalyst.

Comparing the catalytic hydrogenation of ketone catalyzed by complexes 1i and 1j.

A barrier of 19.4 kcal/mol was obtained for Knölker's iron complex catalyzed hydrogenation of acetophenone in our previous calculations. Here, the best modifications (**1i** and **1j**) were used to catalyze the hydrogen transfer of acetophenone, and then compared with Knölker's catalyst, in order to further to verify the catalytic activity of improved iron catalysts.

Fig.6 Free energy ΔG(sol) profile for the hydride transfer of acetophenone catalyzed by iron-complexes **1i** (the upper) and **1j** (the lower) obtained at the M06/6-311+G* level in toluene (kcal/mol), respectively.

Fig.6 shows that both of free energy barriers are lower than 19.4 kcal/mol. The barriers of **2i′TS** and **2j′TS** are separately 15.4 and 16.8 kcal/mol for the hydrogen transfer of $PhCOCH_3$ catalyzed by improved complexes **1i** and **1j**. Based on Eyring equation, k =

$k_B T/h \times e^{-(\Delta G/RT)}$, the rate-constant of **1i** was improved by about 610 times relative to Knölker's catalyst **1a**, which means **1i** possesses higher catalytic activity for the hydrogen transfer of ketones. The other improved catalyst **1j** also shows an increased tendency of catalytic activity, though the rate constant of **1j** is only increased 80 times relative to **1a**. Compared with structures of **2i′TS** and **2j′TS** (see Fig.7), the $PPhH_2$ ligand caused a larger steric hindrance with the closing substrate than PH_3 ligand, which to some extent increased the barrier of the hydrogen transfer. Considering phosphine being a gas, it is difficult to be realistically used for designing catalysts. By contrast, the phenylphosphine ligand is a colorless liquid and can function as a ligand in coordination chemistry, which has a more applicable value in experimental synthesis.

Fig.7 Optimized geometries for **2i′TS** and **2j′TS**. Distances in Å

Conclusions

A variety of improvements on the Knölker's iron-based complex were explored in detail using a DFT method. Hydrogenation of PhCHO catalyzed by Knölker's catalyst was selected as a benchmark due to the fact that it is an actual experimental system. The hydrogen transfer to PhCHO catalyzed by all other modified iron complexes was compared with this benchmark, and some useful conclusions were then obtained.

1. Adding the electron-withdrawing ability of a substituent on the CpOH ring is favorable improving the efficiency of iron catalysts, but increasing its electron donating ability leads to a higher barrier for hydrogenation. The steric factor of this substitution has little influence on the barrier of hydrogenation.

2. Increasing the acidity of CpOH is also an available means for improving catalytic efficiency. But replacing the hydroxyl of CpOH with the amino group is not a valid choice for improvement. The lower acidity of NR′H is kinetically unfavorable to hydrogenation, and the larger steric effects of NR′H rendered the catalytic hydrogen transfer thermodynamically unfeasible.

3. Substituting phosphine ligands for carbonyls is the best method for improving the catalytic activity of the iron catalyst. Here, the substituent of PR_3 must be an electron-donating group rather than an electron-withdrawing group. The steric effect of PR_3 should be controlled in a suitable range. Amongst phosphine ligands both PH_3 and $PPhH_2$ ligands can effectually enhance the catalytic activity for hydrogenation of ketones.

Based on the results of calculations, some available modifications for iron catalysts were obtained and expected to supply some useful suggestions for future experiments. Improvement of the CpOH group is an available method, though it can not significantly increase the catalytic activity of iron complexes for hydrogenation of aldehydes and ketones. In contrast, modification to carbonyl ligands would be a more effective means, especially phosphine ligands replacement.

Notes and references

[a] *Department of Chemical and Materials Engineering, University of Alberta, Edmonton, AB, T6G 2V4, Canada; E-mail: xlu2@ualberta.ca.*

[b] *Computational Center for Molecular Science, College of Chemistry, Nankai University, Tianjin 300071, People's Republic of China; E-mail: zhan1301@purdue.edu.*

[c] *Department of Chemical Engineering Purdue University, West Lafayette, Indiana (USA);*

[d] *Department of Industrial and Physical Pharmacy College of Pharmacy Purdue University, West Lafayette, Indiana (USA); E-mail: tonglei@purdue.edu.*

† Electronic Supplementary Information (ESI) available: [Total electronic energies, thermal corrections to Gibbs free energies and Cartesian coordinates, and so on]. See DOI:

Keywords: iron catalyst; DFT; hydrogenation; improvement.

1 (a) A. Quintard, T. Constantieux and J. Rodriguez, *Angew. Chem., Int. Ed.*, 2013, DOI: 10.1002/anie.201307295. (b) A. K. Steib, T. Thaler, K. Komeyama, P. Mayer and P. Knochel, *Angew. Chem., Int. Ed.*, 2011, **50**, 3303–3307. (c) C. Bolm, J. Legros, J. Le. Paih and L. Zani, *Chem. Rev.*, 2004, **104**, 6217–6254. (d) G. Cahiez, C. Duplais and A. Moyeux, *Org. Lett.*, 2007, **9**, 3253–3254. (e) B. M. Sherry and A. Fürstner, *Acc. Chem. Res.*, 2008, **41**, 1500–1511. (f) S. Enthaler, K. Junge and M. Beller, *Angew. Chem., Int. Ed.*, 2008, **47**, 3317–3321. (g) W. M. Czaplik, M. Mayer and A. Jacobi von Wangelin, *Angew. Chem., Int. Ed.*, 2009, **48**, 607–610. (h) A. Rudolph and M. Lautens, *Angew. Chem., Int. Ed.*, 2009, **48**, 2656–2670. (i) H. U. Blaser, H. Steiner and M. Studer, *ChemCatChem*, 2009, **1**, 210–221.(j) S. Enthaler, *ChemCatChem*, 2010, **2**, 1411–1415. (k) W. Czaplik, M. S. Grupe, M. Mayer and A. Jacobi von Wangelin, *Chem. Commun.*, 2010, **46**, 6350–6352. (l) K. Junge, B. Wendt, N. Shaikh and M. Beller, *Chem. Commun.*, 2010, **46**, 1769–1771. (m) E. Nakamura and N. Yoshikai, *J. Org. Chem.*, 2010, **75**, 6061–6067. (n) G. Cahiez, V. Habiak, C. Duplais and A. Moyeux, *Angew. Chem., Int. Ed.*, 2007, **46**, 4364–4366.

2 K. Junge, K. Schröder and M. Beller, *Chem.Commun.*, 2011, **47**, 4849–4859.

3 B. A. F. L. Bailly and S. P. Thomas, *RSC Adv.*, 2011, **1**, 1435–1445.

4 G. N. Schrauzer, *Chem. Ind.*, 1958, 1403.

5 G. N. Schrauzer, *J. Am. Chem. Soc.*, 1959, **81**, 5307–5310

6 (a) R. Karvemu, R. Prabhakaran and K. Natarajan, *Coord. Chem. Rev.*, 2005, **249**, 911–918. (b) S. Gladiali and E. Alberico, *Chem. Soc.Rev.*, 2006, **35**, 226–236.

7 (a) M. Gomez, S. Jansat, G. Muller, G. Aullon and M. A. Maestro, *Eur. J. Inorg. Chem.*, 2005, 4341–4351. (b) M. Ito, M. Hirakawa, K. Murata and T. Ikariya, *Organometallics*, 2001, **20**, 379–381. (c) K. Abdur–Rashid, S. E. Clapham, A. Hadzovic, J. N. Harvey, A. J. Lough and R. H. Morris, *J. Am. Chem. Soc.*, 2002, **124**, 15104–15118.

8 (a) X. Wu, D. Vinci, T. Ikariya and J. Xiao, *Chem. Commun.*, 2005, 4447–4449. (b) S. E. Clapham and R. H. Morris, *Organometallics*, 2005, **24**, 479–481. (c) M. Martin, E. Sola, S. Tejero, J. L. Andres and L. A. Oro, *Chem. –Eur. J.*, 2006, **12**, 4043–4056. (d) J. Mao and D. C. Baker, *Org. Lett.*, 1999, **1**, 841–843.

9 B. L. Conley, M. K. Pennington–Boggio, E. Boz and T. J. Williams, *Chem. Rev.*, 2010, **110**, 2294–2312.

10 (a) T. C. Johnson, D. J. Morris and M. Wills, *Chem. Soc. Rev.*, 2010, **39**, 81–88. (b) R. M. Navarro, M. A. Peña and J. L. G. Fierro, *Chem. Rev.*, 2007, **107**, 3952–3991. (c) J. A. Turner, *Science*, 2004, **305**, 972–974.

11 V. W. Goldschmidt, *Geochemistry*, Oxford Press, London, 1958, 647.

12 (a) J. W. Peters, W. N. Lanzilotta, B. J. Lemon and L. C. Seefeldt, *Science*, 1998, **282**, 1853–1858. (b) Y. Nicoler, C. Piras, P. Legrand, C. E. Hatchikian and J. C. Fontecilla–Camps, *Structure*, 1999, **7**, 13–23. (c) H. –J. Fan and M. B. Hall, *J. Am. Chem. Soc.*, 2001, **123**, 3828–3829.

13 C. P. Casey and H. R. Guan, *J. Am. Chem. Soc.*, 2007, **129**, 5816–5817.

14 (a) H. –J. Knölker and J. Heber, *Synlett.*, **1992**, 1002-1004. (b) H. –J. Knölker and Heber, J. *Synlett.*, **1993**, 924–926. (c) H. –J. Knölker, E. Baum, H. Goesmann and R. Klauss, *Angew. Chem., Int. Ed.*, 1999, **38**, 2064–2066.

15 Y. Shvo, D. Czarkie, Y. Rahamim and D. F. Chodosh, *J. Am. Chem. Soc.*, 1986, **108**, 7400–7402.

16 M. K. Thorson, K. L. Klinkel, J. M. Wang and T. J. Williams, *Eur. J.*

Inorg. Chem., 2009, 295–302.
17 T. C. Johnson, G. J. Clarkson and M. Wills, *Organometallics*, 2011, **30**, 1859–1868.
18 C. P. Casey and H. R. Guan, *Organometallics*, 2012, *31*, 2631–2638.
19 Y. Blum and Y. Shvo, *Isr. J. Chem.* 1984, **24**, 144–148.
20 C. P. Casey, S. W. Singer, D. R. Powell, R. K. Hayashi and M. Kavana, *J. Am. Chem. Soc.*, 2001, **123**, 1090–1100.
21 C. P. Casey, N. A. Strotman, S. E. Beetner, J. B. Johnson, D. C. Priebe, T. E. Vos, B. Khodavandi and I. A. Guzei, *Organometallics*, 2006, **25***,* 1230–1235.
22 C. P. Casey, S. E. Beetner and J. B. Johnson, *J. Am. Chem. Soc.*, 2008, **130**, 2285–2295.
23 C. P. Casey, and H. R. Guan, *J. Am. Chem. Soc.*, 2009, *131*, 2499–2507.
24 S. E. Clapham, A. Hadzovic and R. H. Morris, *Coord. Chem. Rev.*, 2004, **248**, 2201–2237.
25 L. S. M. Samec, J. –E. Bäckvall, P. G. Andersson and P. Brant, *Chem. Soc. Rev.*, 2006, **35**, 237–248.
26 A. Comas–Vives, G. Ujaque and A. Lledós, *Organometallics*, 2007, **26**, 4135–4144.
27 H. Zhang, D. Chen, Y. Zhang, G. Zhang and J. Liu, *Dalton Trans.*, 2010, **39**, 1972–1978.
28 X. Lu, Y. W. Zhang, P. Yun, M. T. Zhang and T. L. Li, *Org. Biomol. Chem.*, 2013, **11**, 5264–5277.
29 M. J. Frisch, et al. *Gaussian 09*, *Revision B.01*; Gaussian, Inc.: Wallingford, CT, 2009.
30 (a) A. D. Becke, *J. Chem. Phys.*, 1993, **98**, 5648–5652. (b) C. Lee, W. Yang and R. G. Parr, *Phys. Rev. B*, 1988, **37**, 785–789. (c) P. J. Stephens, F. J. Devlin, C. F. Chabalowski and M. J. Frisch *J. Phys. Chem.*, 1994, **98**, 11623–11627.
31 (a) P. J. Hay and W. R. Wadt, *J. Chem. Phys.*, 1985, **82**, 270–283. (b) P. J. Hay and W. R. Wadt, *J. Chem. Phys.*, 1985, **82**, 299–310.
32 (a) K. *J.* Fukui, *Phys. Chem.*, 1970, *74*, 4161–4163. (b) K. Fukui, *Acc. Chem. Res.*, 1981, **14**, 363–368.
33 A. V. Marenich, C. J. Cramer and D. G. Truhlar, *J. Phys. Chem. B*, 2009, **113**, 4538–4543.
34 A. V. Marenich, C. J. Cramer and D. G. Truhlar, *J. Phys. Chem. B*, 2009, **113**, 6378–6396.
35 Y. Zhao and D. G. Truhlar, *Acc. Chem. Res.*, 2008, **41**, 157–167.
36 Y. Zhao and D. G. Truhlar, *Theor. Chem. Account.*, 2008, **120**, 215–241.
37 L. M. Pratt, S. Merry, S. C. Nguyen, P. Quan and B. T. Thanh, *Tetrahedron*, 2006, **62**, 10821–10828.
38 L. M. Pratt, D. G. Truhlar, C. J. Cramer, S. R. Kass, J. D. Thompson and J. D. Xidos, *J. Org. Chem.*, 2007, **72**, 2962–2966.
39 X. Lu, Y. W. Zhang, M. T. Zhang and T. L. Li, *J. Organomet. Chem.*, 2014, **749**, 69–74.
40 S. Kozuch and S. Shaik, *Acc. Chem. Res.*, 2010, **44**, 101–111.

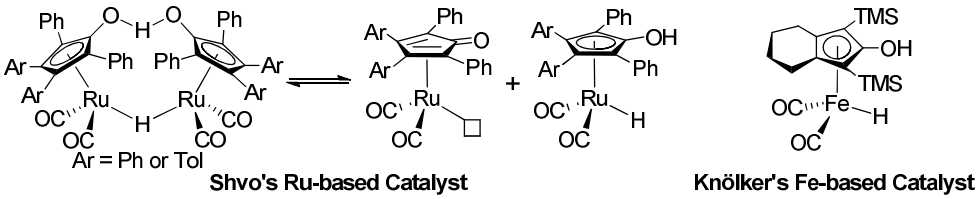

Scheme 1 Shvo's[15] and Knölker's[14] Catalysts

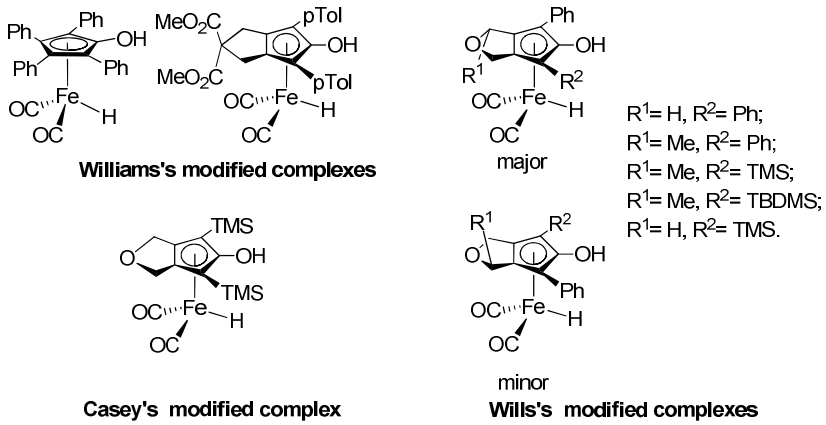

Scheme 2 Some Improved Iron-based Complexes

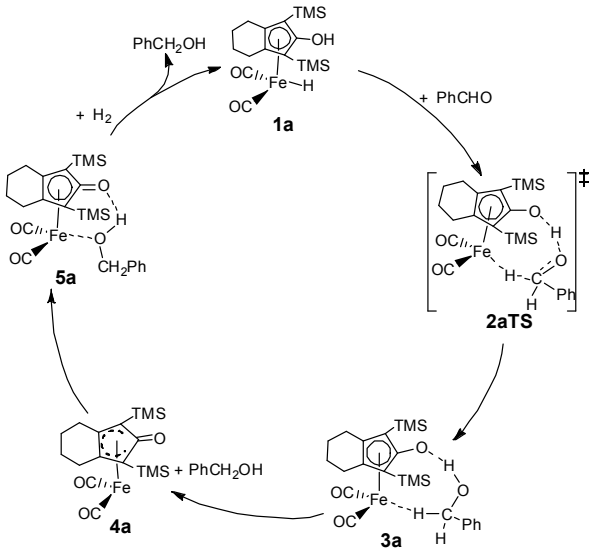

Scheme 3 Hydrogenation mechanism of PhCHO catalyzed by Knölker's Fe-catalyst **1a**

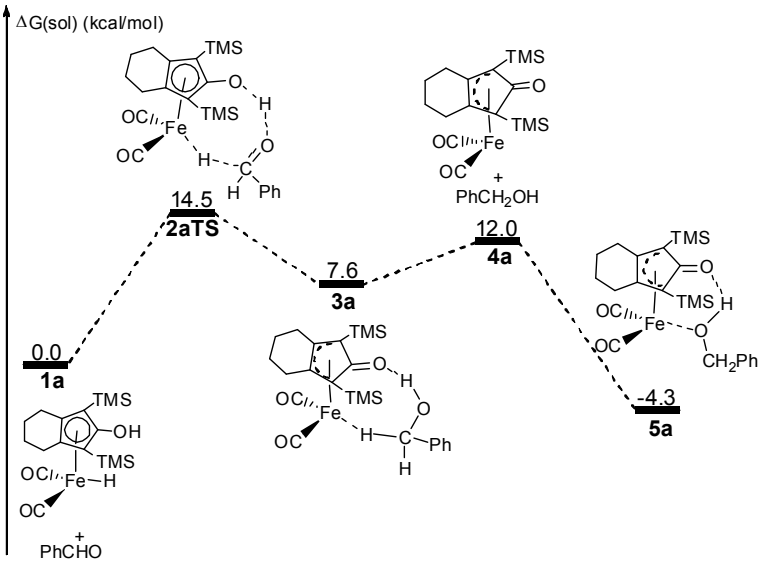

Fig. 1 Free energy Δ*G*(sol) profile for hydrogenation of PhCHO catalyzed by **1a** obtained at the M06/6-311+G* level in toluene (kcal/mol). Relative to free energies of 1a and PhCHO.

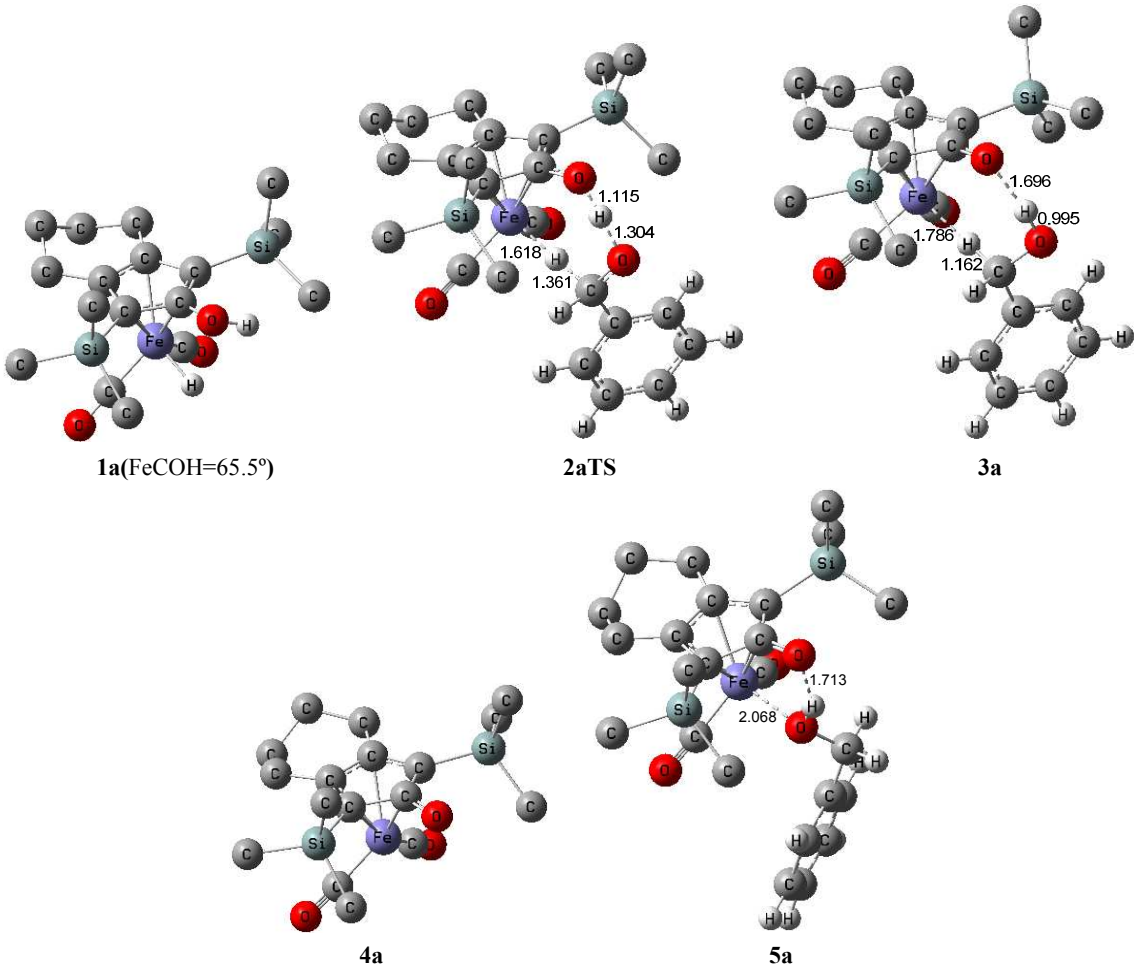

Fig. 2 Optimized structures for hydrogenation of PhCHO catalyzed by **1a**. Distances in Å. FeCOH indicates the dihedral angle. All hydrogen atoms connected to carbons in the CpOH ring were ignored.

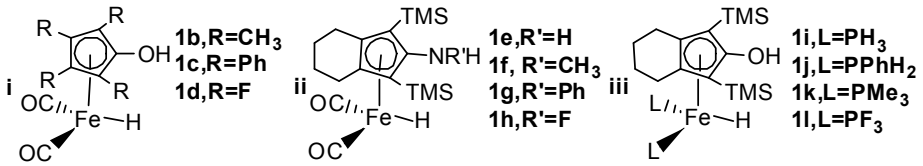

Scheme 4 Designed modifications for the Knölker's catalyst

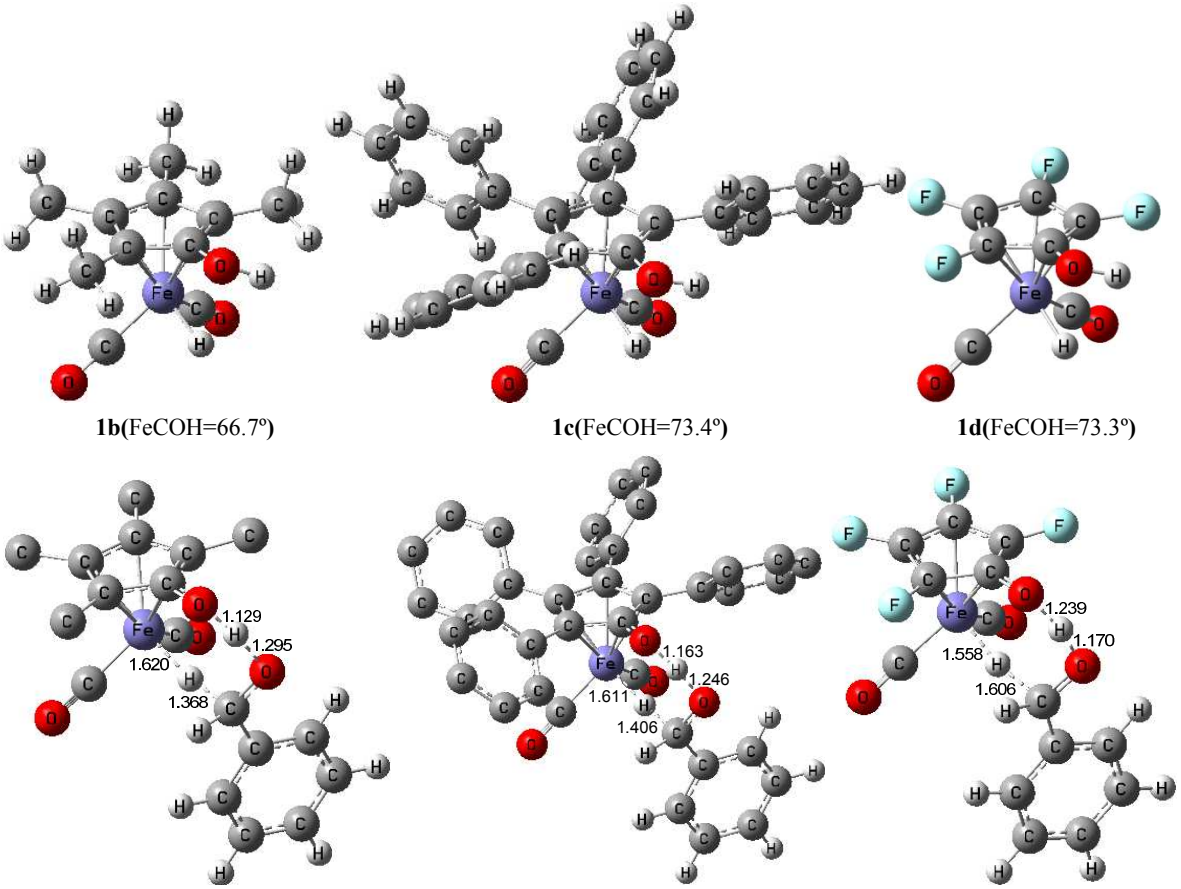

1b(FeCOH=66.7º) **1c**(FeCOH=73.4º) **1d**(FeCOH=73.3º)

2bTS **2cTS** **2dTS**

Fig. 3 Optimized structures for hydrogenation of PhCHO catalyzed by **1b, 1c** and **1d**. Distances in Å. FeCOH indicates the dihedral angle. Hydrogen atoms of the CpOH ring were ignored for only transition states here.

Table 1 Free energy Δ*G*(sol) profiles for hydrogenation of PhCHO catalyzed by improved catalysts **1b, 1c** and **1d** obtained at the M06/6-311+G* level in toluene (kcal/mol).

Catalysts	Δ*G*(sol) (kcal/mol)[a]				
	1+PhCHO	**2TS**	**3**	**4+PhCH$_2$OH**	**5**
1b(R = CH$_3$)	0.0	14.4	5.9	11.4	-5.4
1c (R = Ph)	0.0	14.6	8.6	13.5	-4.2
1d (R = F)	0.0	13.5	3.9	8.3	-9.4

[a] SMD-single-point calculations were performed on the B3LYP-optimized structures in toluene at the theory level of M06/6-311+G*.

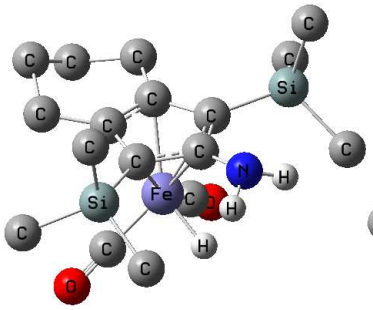

1e(FeCNH(right)=61.8º**)**

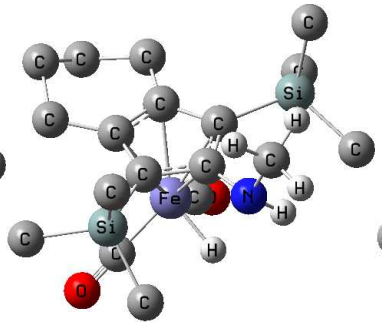

1f (FeCNC(Me)=174.9º**)**

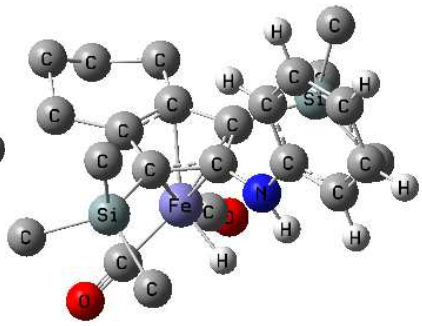

1g(FeCNC(Ph)=172.8º**)**

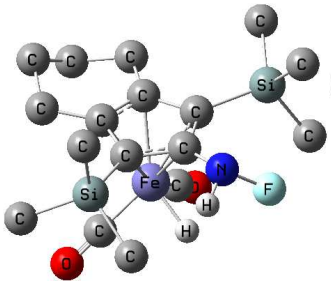

1h(FeCNF=51.5º**)**

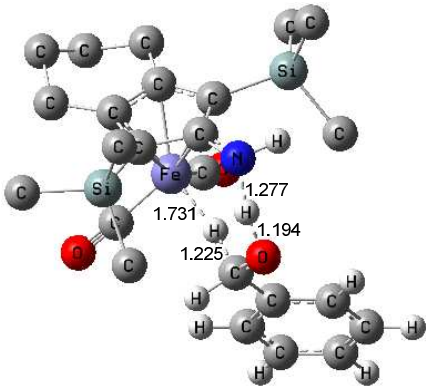

2eTS(H(right)NCC=13.6º**)**

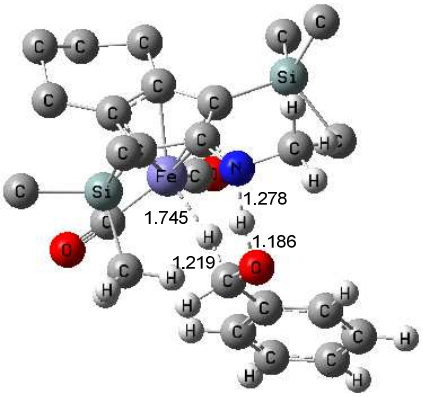

2fTS(C(Me)NCC=30.1º**)**

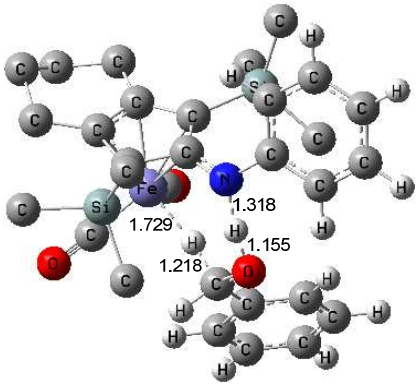

2gTS(C(Ph)NCC=54.4º**)**

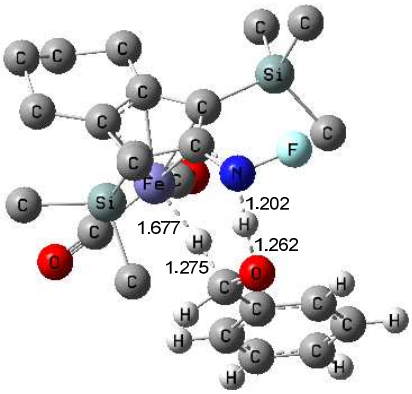

2hTS(FNCC=13.2º**)**

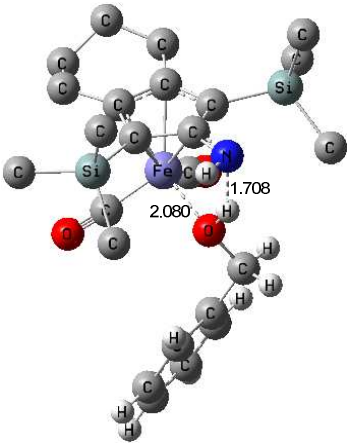

5e(H(left)NCC=15.4º**)**

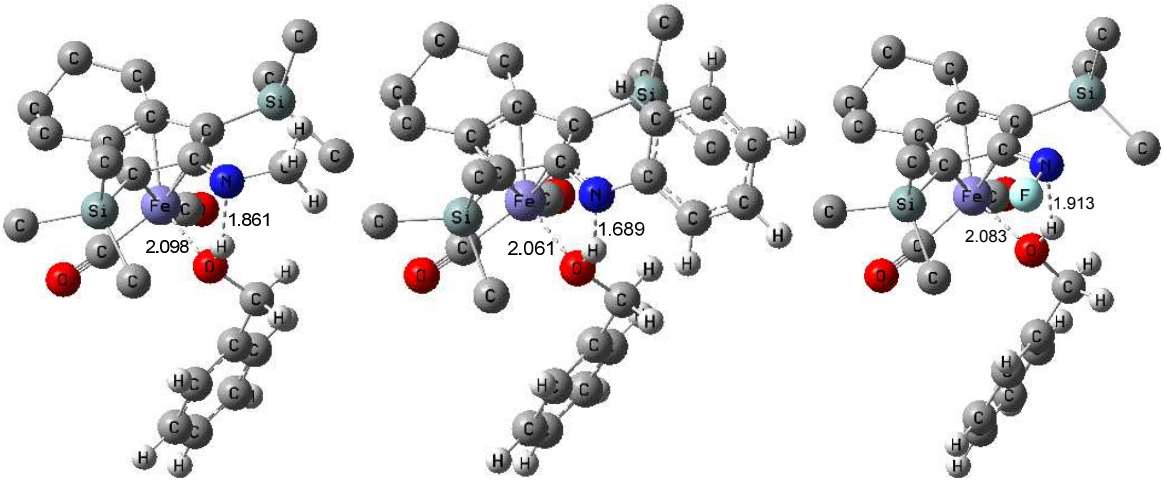

5f(C(Me)NCC=21.1º**)** **5g(**C(Ph)NCC=50.8º**)** **5h(**FNCC=12.3º**)**

Fig. 4 Optimized structures for hydrogenation of PhCHO catalyzed by **1e, 1f, 1g** and **1h** and the dihedral angles. Distances in Å.

Table 2 Free energy Δ*G*(sol) profiles for hydrogenation of PhCHO catalyzed by modifications **1e, 1f, 1g** and **1h** obtained at the M06/6-311+G* level in toluene (kcal/mol).

Catalysts	**Δ*G*(sol) (kcal/mol)[a]**				
	1+PhCHO	**2TS**	**3**	**4+PhCH$_2$OH**	**5**
1e (R = NH_2)	0.0	25.4	24.8	24.8	14.1
1f (R = NCH_3H)	0.0	27.6	26.3	25.2	17.1
1g (R = $NPhH_2$)	0.0	30.2	30.1	27.8	16.8
1h (R = NFH)	0.0	19.5	12.3	15.6	0.4

[a] SMD-single-point calculations were performed on the B3LYP-optimized structures in toluene at the theory level of M06/6-311+G*.

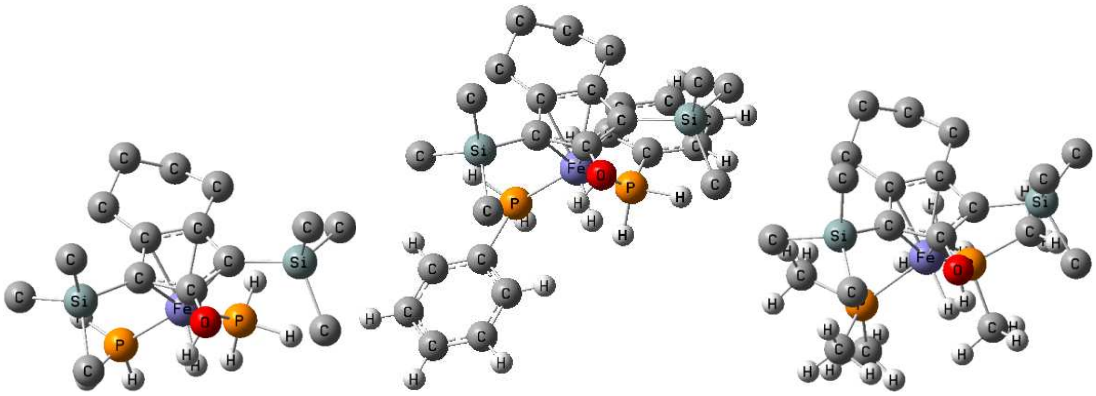

1i(FeCOH=42.9º**)** **1j(**FeCOH=57.6º**)** **1k(**FeCOH=5.8º**)**

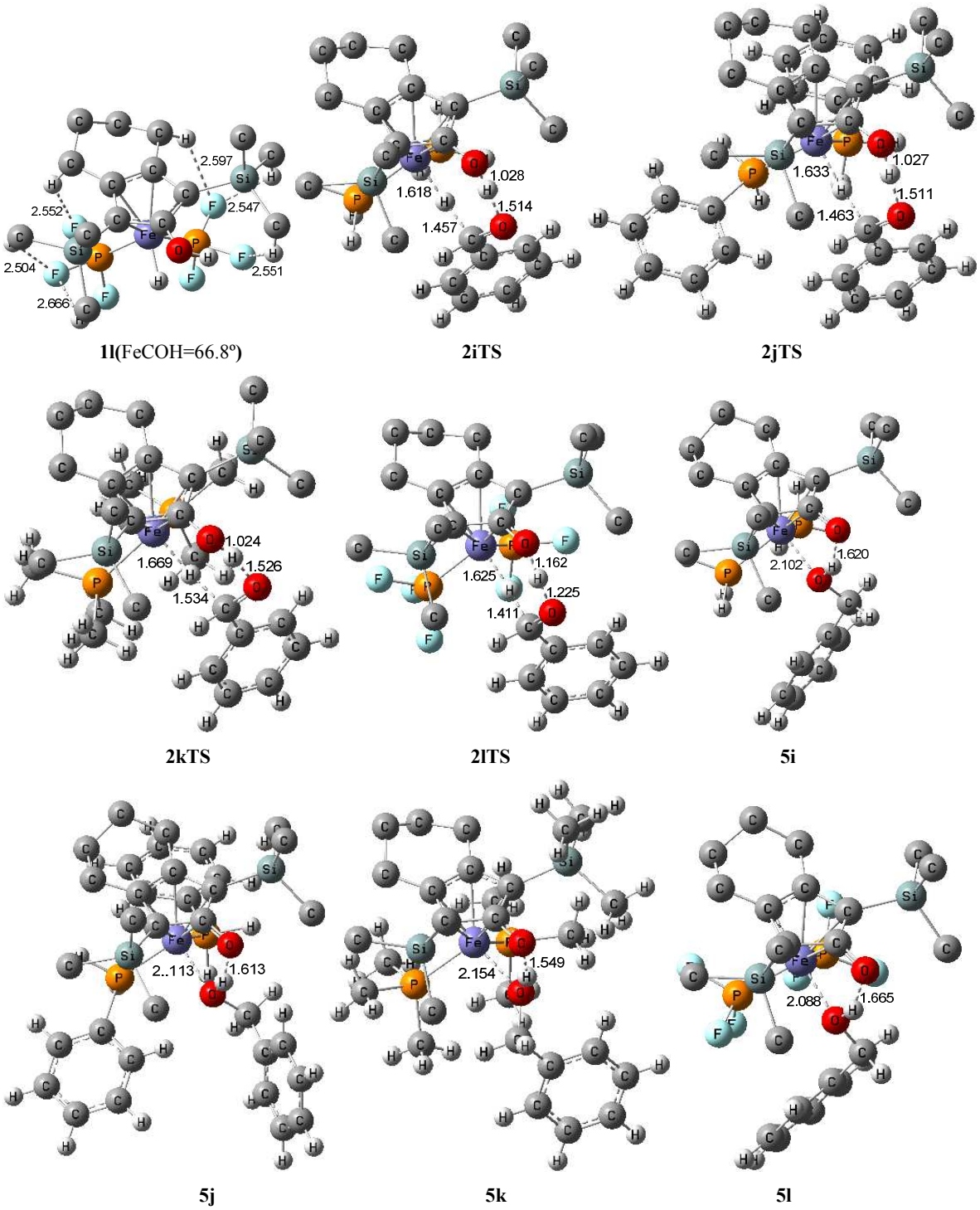

1l(FeCOH=66.8º) **2iTS** **2jTS**

2kTS **2lTS** **5i**

5j **5k** **5l**

Fig. 5 Optimized structures for **1i, 1j, 1k** and **1l** catalyzed hydrogenation of PhCHO and the dihedral angles. Distances in Å.

Table 3 Free energy Δ*G*(sol) profiles for hydrogenation of PhCHO catalyzed by modified catalysts 1i, 1j, 1k and 1l obtained at the M06/6-311+G* level in toluene (kcal/mol).

Catalysts	Δ*G*(sol) (kcal/mol)[a]				
	1+PhCHO	2TS	3	4+PhCH$_2$OH	5
1i (L = PH$_3$)	0.0	8.4	0.9	7.0	-8.1

1j (L = $PPhH_2$)	0.0	11.1	3.6	6.8	-5.1
1k (L = PMe_3)	0.0	13.5	0.2	1.6	-6.6
1l (L = PF_3)	0.0	17.7	10.6	17.2	0.3

[a] SMD-single-point calculations were performed on the B3LYP-optimized structures in toluene at the theory level of M06/6-311+G*.

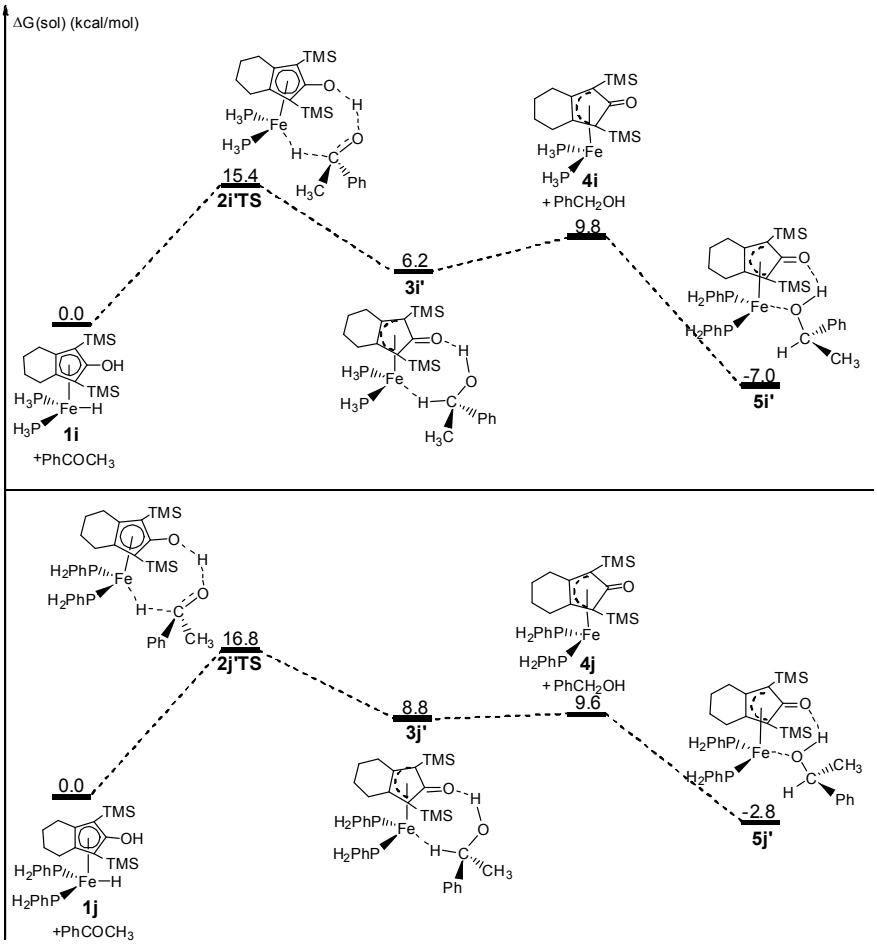

Fig. 6 Free energy Δ*G*(sol) profile for the hydride transfer of acetophenone catalyzed by iron-complexes **1i** (the upper) and **1j** (the lower) obtained at the M06/6-311+G* level in toluene (kcal/mol), respectively.

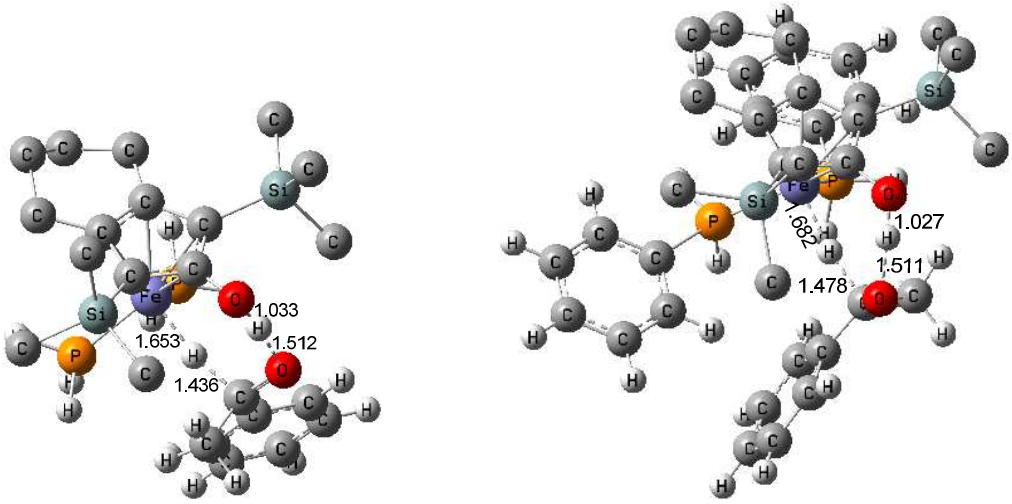

2i′TS **2j′TS**

Fig. 7 Optimized geometries for **2i′TS** and **2j′TS**. Distances in Å